Poly-L-Arginine Enhances Paracellular Permeability via Serine/Threonine Phosphorylation of ZO-1 and Tyrosine Dephosphorylation of Occludin in Rabbit Nasal Epithelium

Kazuo Ohtake,[1] Takuya Maeno,[1] Hideo Ueda,[1] Masahiko Ogihara,[1] Hideshi Natsume,[1,2,3] and Yasunori Morimoto[1,2]

Received May 9, 2003; accepted July 9, 2003

Purpose. The purpose of the present study is to explore whether a poly-L-arginine (poly-L-Arg)-induced increase in tight junctions (TJ) permeability of fluorescein isothiocyanate-labeled dextran (MW 4.4 kDa, FD-4) is associated with the Ca^{2+}-dependent signaling and occurs following the phosphorylation/dephosphorylation of TJ proteins.
Methods. Excised rabbit nasal epithelium was mounted in an Ussing-type chamber for measurement of FD-4 transport and membrane conductance (Gt) in the presence of various inhibitors that are involved in the Ca^{2+}-dependent pathway and the phosphorylation/dephosphorylation of TJ proteins. The resultant distribution of TJ proteins was observed using confocal laser scanning microscopy (CLSM) in an immunostaining.
Results. The increase in TJ permeability of FD-4 induced by 0.2 mg/ml poly-L-Arg was not altered by treatment with inhibitors of possible Ca^{2+} mobilization pathways followed by exposure of poly-L-Arg, suggesting that the promoting effect of poly-L-Arg is independent of Ca^{2+}-related signaling. On the other hand, the protein kinase C (PKC) and tyrosine phosphatase inhibitors suppress the increase in TJ permeability by poly-L-Arg, indicating that serine/threonine phosphorylation by way of Ca^{2+}-independent PKC and tyrosine dephosphorylation of junction proteins may have occurred. Furthermore, immunofluorescent monitoring of ZO-1, a TJ associated protein, and occludin, an integral membrane protein localizing at TJ, after preincubation with PKC and tyrosine phosphatase inhibitors followed by poly-L-Arg treatment has shown that the internalization of ZO-1 and occludin occurred by way of serine/threonine phosphorylation by PKC activation and by way of tyrosine dephosphorylation, respectively, providing TJ disassembly.
Conclusions. We conclude that poly-L-Arg enhances the paracellular permeability of FD-4 (i.e., macromolecules), at least, by way of both serine/threonine phosphorylation of ZO-1 and tyrosine dephosphorylation of occludin in rabbit nasal epithelium.

KEY WORDS: poly-L-arginine; ZO-1; occludin; PKC; tyrosine phosphatase; transnasal drug delivery system.

[1] Faculty of Pharmaceutical Sciences, Josai University, 1-1 Keyakidai, Sakado, Saitama 350-0295, Japan.
[2] Research Institute of TTS Technology, 1-1 Keyakidai, Sakado, Saitama 350-0295, Japan.
[3] To whom correspondence should be addressed. (e-mail address: natsume@josai.ac.jp)

ABBREVIATIONS: poly-L-Arg, poly-L-arginine; TJ, tight junction; PKC, protein kinase C; FD-4, fluorescein isothiocyanate-labeled dextran (MW 4.4 kDa,); $[Ca^{2+}]_i$, intracellular Ca^{2+} concentration; RTK, receptor tyrosine kinase; MLCK, myosin light chain kinase; MEK, mitogen-activated protein kinase; RhoK, Rho-associated kinase; PI3K, phosphatidylinositol 3-kinase; BRS, bicarbonated Ringer's solution; PD, potential difference; Isc, short-circuit current; TEER, transepithelial electrical resistance; Gt, membrane conductance; CLSM, confocal laser scanning microscopy; TBS, tris-buffered saline; Papp, apparent permeability coefficient.

INTRODUCTION

Tight junctions (TJ) are the most apical structures of the junction complexes in epithelial and endothelial cell sheets. Integral membrane proteins, occludin, claudin, and junctional adhesion molecule (JAM) and intracellular junction associated proteins, ZO-1, ZO-2, ZO-3, and 7H6 localize at TJ and constitute TJ strand network (1–4). TJ serve as a primary permeability barrier regulating the diffusion of ions and small molecules by way of the paracellular pathway ("gate function") and restricting the lateral diffusion of membrane lipids and proteins between the apical and basolateral compartments to maintain cell polarity ("fence function") (1,2). Most small drug molecules are transported by way of the transcellular pathway by passive diffusion and active transport, easily entering the systemic circulation and distributing to various tissues in the body, hence the minor contribution of the paracellular pathway. Many researchers have shown that extremely small amounts of macromolecules penetrate epithelial cellular sheets and consequently the paracellular route is the predominant pathway because of its hydrophilic nature, large molecular dimensions, and no major partitioning into cell membranes (3,4). Thus, it is not easy to deliver large hydrophilic molecules such as bioactive peptides, hormones, vaccines, and genes by way of the transmucosal routes into the systemic circulation. It seems a convenient approach to produce a transient reduction in barrier function of TJ to deliver large amounts of these compounds without disruption of epithelial cellular sheets.

Recently, it has been shown that polycationic materials such as poly-L-arginine (5,6), poly-L-lysine (5), protamine (7), chitosan (8,9) and *N*-trimethyl chitosan (10) have the potential to promote transmucosal delivery of macromolecules without producing severe epithelial toxicity. Ohtake *et al.* found that nasal absorption of a model hydrophilic compound fluorescein isothiocyanate-labeled dextran (MW 4.4 kDa, FD-4) increased because of a transient opening of cell-to-cell junctions following co-administration of poly-L-arginine (MW 42.4 kDa, poly-L-Arg) *in vivo* in rats (11). They have also characterized the enhancing effect of poly-L-Arg on the transport of FD-4 across the excised rabbit nasal epithelium *in vitro* (12). Poly-L-Arg predominantly exhibits enhanced paracellular solute transport involving alteration in the distribution of TJ proteins, ZO-1, occludin and adherens junction protein E-cadherin, and acts only on the apical membrane component (12). The enhancing effect of poly-L-Arg was significantly inhibited in the presence of either 1 mM 2,4-dinitrophenol, or 1 mM ouabain, suggesting that the poly-L-Arg-induced increase in paracellular permeability, is dependent on metabolic energy (cell viability) and energy-dependent cellular events (12). Other polycations, especially chitosan, have been also characterized in terms of the predominantly paracellular transport of solutes, TJ disassembly and energy-dependence of cellular events (9,13). These results suggest that polycations may induce intracellular signaling resulting in the altered distribution of junction proteins, even although the processes induced by these materials are different. However, to date, the regulatory mechanism for polycations including poly-L-Arg-induced epithelial TJ permeability remains unknown. Poly-L-Arg had been shown to activate some kinases and/or phosphatases in various cell

0724-8741/03/1100-1838/0 © 2003 Plenum Publishing Corporation

lines (14–16), but these activation processes are unrelated to the increase in paracellular solute transport by poly-L-Arg.

In the present study, we provide the first evidence for the regulatory mechanism of the poly-L-Arg-induced increase in TJ permeability across the excised rabbit nasal epithelium based on the change in FD-4 permeability, membrane conductance (Gt) and TJ localization in the presence of various inhibitors that are involved in the Ca^{2+}-dependent pathway and the phosphorylation/dephosphorylation of TJ proteins.

MATERIALS AND METHODS

Materials

FD-4, poly-L-Arg hydrochloride (MW ca. 42.4 kDa) and normal goat serum were purchased from Sigma Chemical Co., Ltd. (St Louis, MO, USA). SK&F 96365, thapsigargin, genistein, PP2, W-7, PD98059, LY294002, rottlerin, Gö 6983, okadaic acid, and dephostatin were obtained from Calbiochem (San Diego, CA, USA). Nifedipine, fluo 3-AM and A23187 were obtained from Wako Pure Chemical Industries (Osaka, Japan). Y27632 was a gift from Welfide (Osaka). Mouse anti-ZO-1 monoclonal antibodies and mouse anti-occludin monoclonal antibodies were obtained from Zymed (San Francisco, CA). FITC-conjugated goat affinity purified antibody to mouse IgG was obtained from ICN Biomedicals (Irvine, CA). All other chemicals were of reagent grade.

Nasal Tissue Preparation and Transfer to the Ussing Chamber

The method has been fully described previously (12). Briefly, male Japanese white rabbits (Tokyo Laboratory Animals, Tokyo, Japan), weighing 2.5–3.0 kg were sacrificed by slowly increasing the CO_2 concentration in a CO_2 gas animal euthanasia cabinet (KN-750-1, Natsume Co., Ltd, Tokyo) according to the NIH standards as described in "Principles of Laboratory Animal Care". The nasal septum was then gently removed and, after trimming, the excised nasal epithelium was carefully mounted in the tissue adapter with a circular aperture of 0.5 cm^2. The adapter-tissue assembly was then placed between two halves of Ussing chambers maintained at 37 ± 1°C. The bathing solution, bicarbonated Ringer's solution (BRS, 4 ml on each side) was bubbled with 95% O_2/5% CO_2 to maintain the pH at 7.4. BRS consisted of 125 mM NaCl, 5 mM KCl, 10 mM $NaHCO_3$, 1.2 mM NaH_2PO_4, 1.4 mM $CaCl_2$, and 11 mM D-glucose.

Measurement of Bioelectric Parameters

All experiments were performed under open-circuit conditions with intermittent short-circuit conditions using a short-circuit current amplifier (CEZ-9100, Nippon Koden, Tokyo, Japan). The potential difference (PD) was measured with two matched calomel electrodes. Two salt-agar bridges (containing 3% agar in 4M KCl), the tips of which were located near the center of the tissue surfaces, were used to connect electrically the reservoir fluids to the electrode wells. The electrical output of the calomel electrodes was amplified by the voltage-clamp unit. The direct current across the tissue was transmitted by way of a pair of matched Ag/AgCl electrodes with conducting agar bridges, with the tips positioned away from the tissue surfaces at the far ends of the reservoirs. The short-circuit current (Isc) flowing in the bath-tissue-bath current was monitored at 15 min intervals. Transepithelial electrical resistance (TEER) was calculated as follows: TEER = PD/(Isc × A) according to Ohm's law, where A is the effective permeation area (0.5cm^2). Prior to each experiment, the solution resistance (<100 Ω cm^2) was compensated for the automatic voltage clamp unit. A baseline PD of 5.5 ± 0.6 mV, an Isc of 96 ± 19 μA / cm^2 and a TEER of 57.2 ± 5.1 Ω · cm^2 were observed for 108 nasal mucosae, comparable with our previous values (12). The TEER obtained every 15 min was converted to membrane conductance (Gt = 1/TEER) to give an indication of the paracellular permeability. Baseline Gt, inhibitor-induced Gt, and poly-L-Arg-induced Gt were calculated and averaged from the steady-state portion. To evaluate the effect of each inhibitor and poly-L-Arg on Gt, the Gt ratio was calculated as follows:

$$\text{Gt ratio} = \text{inhibitor-induced Gt or poly-L-Arg-induced Gt / baseline Gt} \quad (1)$$

Transport Study

After the bioelectric parameters PD, Isc, and TEER for the nasal epithelium had equilibrated, apical and basolateral bathing fluids were replaced with fresh BRS to minimize possible enzymatic degradation of poly-L-Arg (11,12). Solute transport was initiated by adding FD-4 (final concentration 2.5 mg/ml) to the apical bathing solution. An aliquot (0.5 ml) was sampled from the basolateral side at 15 min intervals. After 90 min, the nasal epithelium was then treated with one of the following inhibitors: thapsigargin (1 μM) (17,18) for 45 min, nifedipine (50 μM) (17,18) for 45 min, SK&F 96365 (100 μM) (19) for 75 min, genistein (30 μM) (20) for 75 min, PP2 (50 μM) (21) for 45 min, W-7 (100 μM) (22) for 90 min, Y27632 (100 μM) (23) for 75 min, PD98059 (50 μM) (24) for 75 min, LY294002 (50 μM) (25) for 75 min, rottlerin (100 μM) (26) for 60 min, Gö 6983 (10 μM) (27) for 60 min, okadaic acid (0.1 μM) (28) for 60 min, dephostatin (50 μM) (29) for 60 min in apical side. These concentrations are 10~100-fold higher than the reported IC_{50} (17–29), allowing sufficient inhibition under our experimental condition. Transport study was also conducted in the presence of high concentration of Ca^{2+} (4.2 mM; 1.4 mM in normal BRS) in both apical and basolateral bathing fluids to examine whether extracellular Ca^{2+} in relation to the poly-L-Arg effect. The nasal epithelium was then exposed to poly-L-Arg (final concentration 0.2 mg/ml) for 120 min. The apparent permeability coefficient (Papp) of FD-4 was calculated using the following Eq. (2):

$$\text{Papp (cm/sec)} = dQ/dt \times 1/A \times C_0 \quad (2)$$

where dQ/dt (μg/sec) is estimated from the steady-state portion of the slope of the cumulative amount of FD-4 in the receiver fluid vs. time, C_0 (μg/ml) is the initial FD-4 concentration on the donor side, and A (cm^2) is the effective surface area of the nasal epithelium. Baseline Papp, inhibitor-induced Papp, and poly-L-Arg-induced Papp were calculated from Eq. (2). To evaluate the effect of each inhibitor and poly-L-Arg on the baseline Papp of FD-4, the Papp ratio was calculated as follows:

$$\text{Papp ratio} = \text{inhibitor-induced Papp or poly-L-Arg-induced Papp / baseline Papp} \quad (3)$$

FD-4 Assay

One hundred microliters of sample solution was diluted 50-fold with 0.2 M potassium dihydrogenphosphate-0.2 M sodium borate buffer (pH 8.5). The fluorescence of FD-4 was determined in a fluorescence spectrofluorometer (RF-5000, Shimadzu, Kyoto, Japan) at an excitation wavelength of 495 nm and an emission wavelength of 515 nm.

Measurement of Intracellular Ca^{2+} Concentration ($[Ca^{2+}]_i$) in Confocal Laser Scanning Microscopy

The isolated nasal epithelia were cut into small pieces (4–5 mm^2), incubated with BRS which was bubbled with 95% O_2 / 5% CO_2 for 60 min at 37°C in a Petri dish. Thereafter, small pieces were incubated with 5 μM fluo 3-AM as a free Ca^{2+} indicator in BRS for 60 min at 37°C. After incubation, these samples were rinsed twice with BRS for 15 min, and transferred to a Petri dish filled with fresh BRS (4 ml). Poly-L-Arg (0.2 or 2 mg/ml) or A23187 (1 μM) was then added to the Petri dish. Immediately, these samples were subjected to CLSM using an MRC-600 Lasersharp System (Bio-Rad Laboratories, Richmond, CA, USA) linked to a Zeiss Axioplan equipped with a water immersion objective (x 40, NA 0.80, Achroplan, Carl Zeiss, Oberkochen, Germany). The fluorescence of fluo 3 was excited at an Argon laser wavelength of 488 nm. The dynamic changes in intensity in the nasal epithelial cells were monitored and recorded every 15 s. The data obtained are expressed as relative values because of the error inherent in single-wavelength detection of fluorometric intensities. A relative fluorescence value was calculated from the following Eq. [4]:

$$\text{Relative fluorescence} = (F–BG)/(F_0–BG) \qquad (4)$$

where F and F_0 are the intensity of the fluorescence at each time point and at time zero, respectively, and BG is the background fluorescence.

Immunolocalization

The method has been fully described previously (12). Briefly, the nasal epithelium treated under various conditions was removed from the Ussing chamber, rinsed three times with pH 7.4 tris buffered saline (TBS, 50 mM tris-HCl, 150 mM NaCl) for 15 min, fixed in 3.75% formalin – TBS for 10 min at room temperature, and permeabilized by 0.25% Triton X-100 in TBS for 50 min at room temperature. The tissue was then incubated for 30 min with 50% normal goat serum in TBS and with 1:100 mouse anti-ZO-1 antibodies or 1:100 mouse anti-occludin antibodies in TBS overnight at 4°C. After rinsing in TBS, the tissue was then incubated with 1:50 FITC-conjugated goat antibody to mouse IgG for 120 min. After rinsing, the labeled tissue was cut into small pieces (4–5 mm^2) and mounted between a glass slide and coverslip. The fluorescence of these proteins in the nasal epithelium was then observed using an MRC-600 Lasersharp system with an oil immersion objective (x 63, NA 1.25, Zeiss Neofluar, Carl Zeiss) and excited at an Argon laser wavelength of 488 nm. A composite picture of 20 sections (0.2 μm apart on the z axis) of each membrane was collected for analysis.

Statistics

Statistical analyses were performed using Student's *t* test. A p value of 0.05 was considered significant.

RESULTS

Influence of Poly-L-Arg on Intracellular and Extracellular Ca^{2+} Disposition

To verify effect of poly-L-Arg on intracellular Ca^{2+} disposition, FD-4 permeation across the excised nasal epithelium and TEER were determined following treatment with various $[Ca^{2+}]_i$-related inhibitors at the apical side. As shown in Fig. 1b, treatment of poly-L-Arg following incubation with

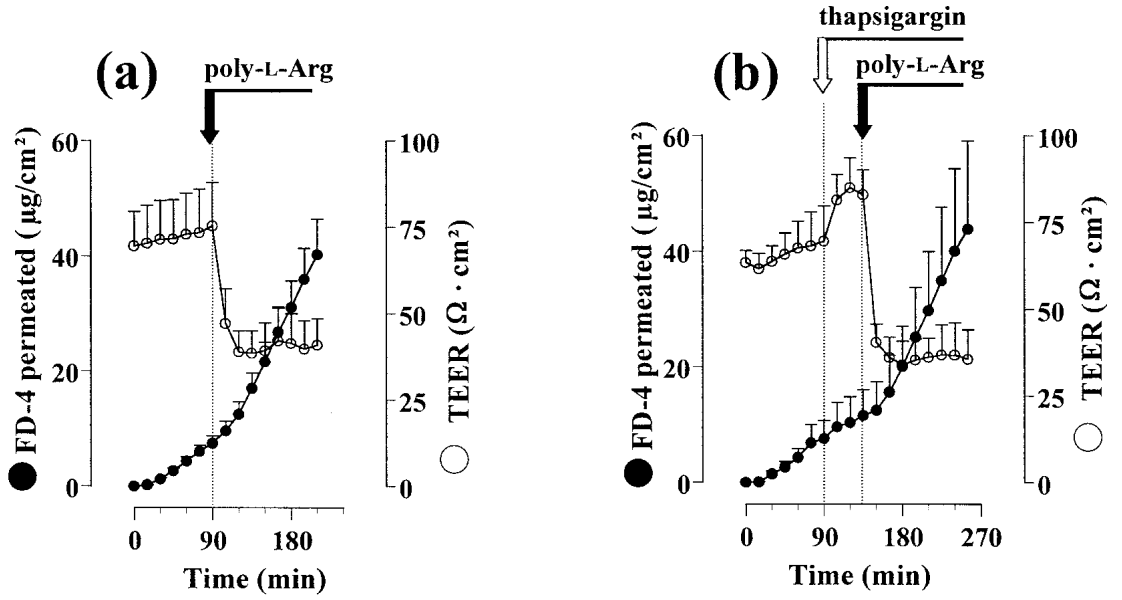

Fig. 1. Effect of 0.2 mg/ml poly-L-Arg on FD-4 permeation and TEER in the presence (b) and absence (a) of 1 μM thapsigargin in the rabbit nasal epithelium. (Closed arrow) Apical application of poly-L-Arg. (Open arrow) Apical application of thapsigargin. Data represent mean ± SE (n = 4).

thapsigargin (1 μM), a selective inhibitor for reticular Ca^{2+}-ATPase (17,18), produced an increase in FD-4 permeation with a concurrent decrease in TEER. The Papp of FD-4 achieved by poly-L-Arg in the presence of thapsigargin was 2.5-fold that of the control value (calculated over 30 to 90 min) of $7.74 \pm 2.89 \times 10^{-7}$ cm/s, and TEER was reduced to 55.1% of that at baseline, 65.7 ± 6.63 Ω·cm^2. These trends were almost identical to those found after exposure of poly-L-Arg alone (see Fig. 1a), suggesting that poly-L-Arg had no effect on Ca^{2+} release from the endoplasmic reticulum.

To measure the effect of poly-L-Arg on Ca^{2+} entering by way of the plasma membrane, the nasal epithelium was incubated with SK&F 96365 (100 μM), a receptor-activated Ca^{2+} channel inhibitor (19), or nifedipine (50 μM), an L-type Ca^{2+} channel inhibitor (17,18), followed by addition of poly-L-Arg on the apical side. Figures 2a–d show the effect of various inhibitors including thapsigargin on the increase in Papp of FD-4 and Gt (1/TEER) induced by poly-L-Arg. After treatment with inhibitors alone, the ratios of Papp and Gt were almost identical compared with no treatment with inhibitor (ratio ≒ 1, see Fig. 2a–d, solid bar) also, these inhibitors did not affect the increase in Papp and Gt induced by poly-L-Arg (see Fig. 2a–d, open bar). To ascertain that no induction of $[Ca^{2+}]_i$ was possible via other Ca^{2+}-related pathways by poly-L-Arg, differential changes in the fluorescence of intracellular fluo 3 were measured following the addition of fluo 3-AM to the outer medium. As shown in Fig. 3, A23187 (1 μM), a calcium ionophore, led to a transient increase in the relative ratio of fluorescence (see Fig. 3c), whereas 0.2 and 2 mg/ml poly-L-Arg did not significantly alter these ratios (see Fig. 3a,b). These results indicate strongly that the action of poly-L-Arg, leading to increased paracellular permeability of FD-4, is unrelated to the change in $[Ca^{2+}]_i$ produced by the entry of extracellular Ca^{2+} across the major calcium channels in the epithelial membrane. Furthermore, high concentration of Ca^{2+} (4.2 mM; 1.4 mM in normal BRS) in both the apical and basolateral bathing fluids also had no effect on the poly-L-Arg-induced Papp and Gt (see Fig. 2e). This suggests that there is no relationship between poly-L-Arg action and the displacement or clearance of Ca^{2+} from the intercellular junctions.

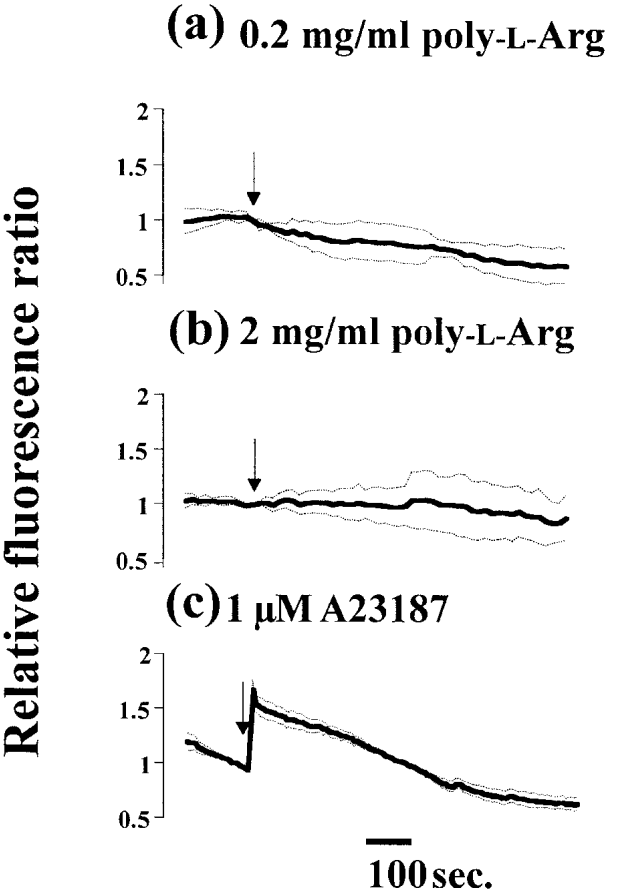

Fig. 3. Effect of A23187 and poly-L-Arg on $[Ca^{2+}]_i$ response in the rabbit nasal epithelium. (Arrows) Application of poly-L-Arg or A23187. Data represent mean ± SE (n = 6).

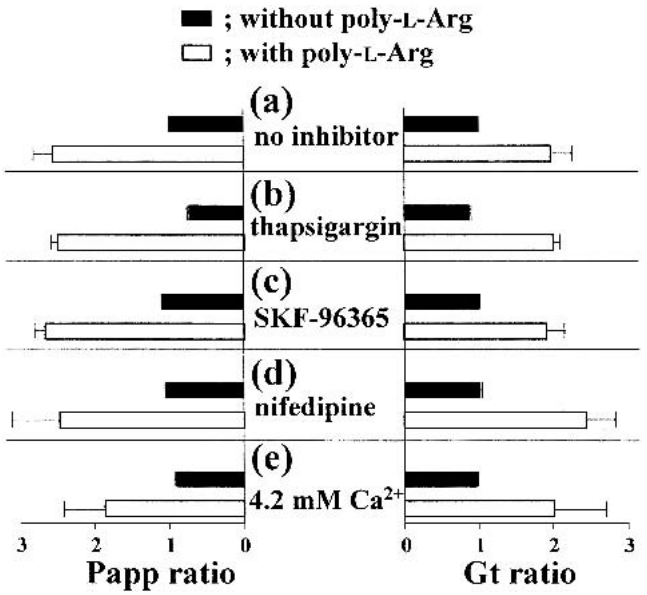

Fig. 2. Effect of Ca^{2+}-mobilization inhibitors and high concentration of Ca^{2+} (4.2 mM) in both apical and basolateral bathing fluids on Papp of FD-4 and Gt induced by poly-L-Arg in the rabbit nasal epithelium. Data represent mean ± SE (n = 4).

Contribution of Kinases or Phosphatases

The effect of kinase and phosphatase on the increase in Papp of FD-4 and Gt induced by poly-L-Arg was shown in Fig. 4. Treatment with inhibitor alone did not influence the ratio of Papp and Gt (see Fig. 4, solid bar). Of these inhibitors, W-7 for myosin light chain kinase (MLCK) (100 μM) (22), Y27632 for Rho-associated kinase (RhoK) (100 μM) (23), PD98059 for mitogen-activated protein kinase (MEK) (50 μM) (24), LY294002 for phosphatidylinositol 3-kinase (PI3K) (50 μM) (25), genistein for receptor tyrosine kinase (RTK) (30 μM) (20), PP2 for non-RTK inhibitor (50 μM) (21), and okadaic acid for serine/threonine phosphatase inhibitor (0.1 μM) (28) did not alter the poly-L-Arg-induced Papp of FD-4 and Gt (see Fig. 4, open bar). On the other hand, poly-L-Arg-induced Papp was significantly suppressed by the PKC inhibitor, rottlerin (100 μM) (26) and Gö 6983 (10 μM) (27), whereas poly-L-Arg-induced Gt trended to be reduced slightly (although the difference was not significant). In addition, both the poly-L-Arg-induced Papp and Gt were significantly reduced by the tyrosine phosphatase inhibitor dephostatin (50 μM) (29). These results suggest that poly-L-Arg

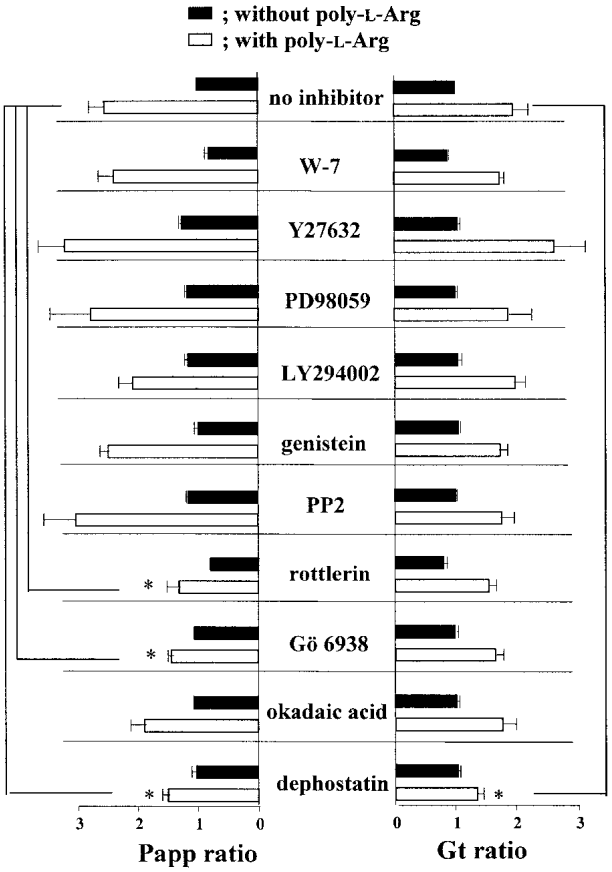

Fig. 4. Effects of various kinase and phosphatase inhibitors on Papp of FD-4 and Gt induced by poly-L-Arg in the rabbit nasal epithelium. Data represent mean ± SE (n = 4) with *p < 0.05.

leads to activation of PKC and tyrosine phosphatase as far as the increased Papp of FD-4 and Gt are concerned.

Immunofluorescent Localization of Tight Junction Proteins ZO-1 and Occludin

Figure 5 shows the immunofluorescent localization of ZO-1 and occludin. In the control epithelium, both ZO-1 and occludin were present in the cellular periphery and appeared as a continuous band localized at the intercellular borders (see Fig. 5a and b). Following exposure to poly-L-Arg on the apical side at a concentration of 0.2 mg/ml for 120 min, the immunofluorescence of both ZO-1 and occludin appeared to be dispersed into the cytoplasm (see Fig. 5c and d), suggesting that poly-L-Arg alters the distribution of junction proteins including ZO-1 and occludin involving the enhancement of paracellular solute transport in the excised rabbit nasal epithelium as shown by our previous results (12).

Following incubation with rottlerin (100 μM) (26), Gö 6983 (10 μM) (27) and dephostatin (50 μM) (29) for 60 min, respectively (treatment with inhibitor alone), the localization of ZO-1 and occludin was almost identical to the control (see Fig. 5e, f, i, j, m and n). On the other hand, when the nasal epithelium was treated with 0.2 mg/ml poly-L-Arg following rottlerin exposure, the immunofluorescence of occludin at the cell-to-cell contact region seemed to be uniformly dispersed in the cytoplasm, whereas ZO-1 was still present in these regions (see Fig. 5g and h). A similar phenomenon was observed after exposure of Gö 6983 (10 μM) to 0.2 mg/ml poly-L-Arg (see Fig. 5k and l).

In contrast to the findings with rottlerin and Gö 6983, following treatment of dephostatin with 0.2 mg/ml poly-L-Arg, most of the ZO-1 disappeared from the cell-to-cell contact region, whereas most of the occludin remained (see Fig. 5o and p). Overall, these results suggest that poly-L-Arg alters the distribution of ZO-1 and occludin by way of serine/threonine phosphorylation involving PKC activation and tyrosine dephosphorylation, respectively, providing TJ disassembly, and thereby increasing the paracellular transport of FD-4.

DISCUSSION

In the present study, we investigate whether a poly-L-Arg-induced increase in TJ permeability is associated with Ca^{2+}-dependent signaling and occurs by the phosphorylation/dephosphorylation of TJ proteins. These processes are well known to regulate the paracellular permeability of various epithelia (17,18,20–25,28,30,31).

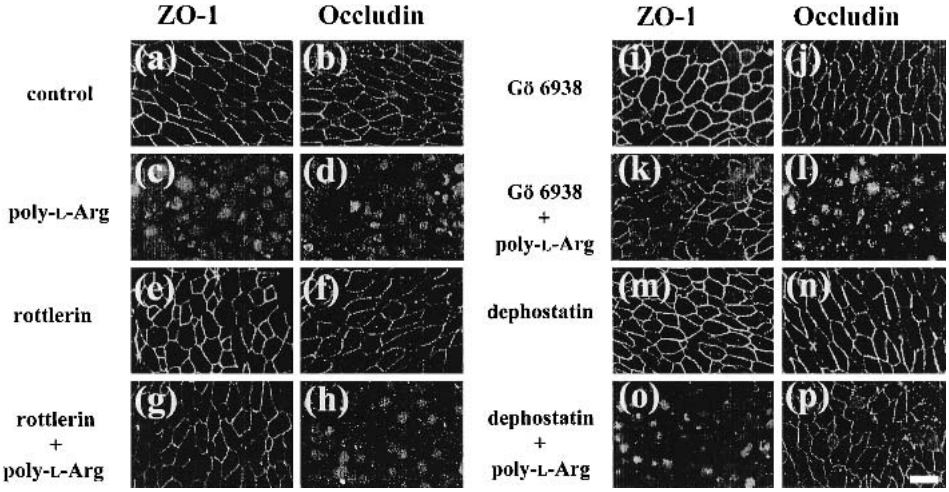

Fig. 5. Effects of PKC and tyrosine phosphatase inhibitors on poly-L-Arg-induced immunofluorescent localization of ZO-1 and occludin in the rabbit nasal epithelium. Scale bar: 15 μm.

In excised rabbit nasal epithelium, the increase in TJ permeability of FD-4 induced by poly-L-Arg was not altered by treatment with inhibitors or blockers of the $[Ca^{2+}]_i$ mobilization pathways (see Figs. 1 and 2). Furthermore, treatment with poly-L-Arg at a concentration of 0.2 mg/ml resulted in no significant change in $[Ca^{2+}]_i$ (see Fig. 3), unrelated to the $[Ca^{2+}]_i$ mobilization of poly-L-Arg effect. This was confirmed by measuring the effect of poly-L-Arg on MLCK activation stimulated by Ca^{2+}-calmodulin complex where increases in intracellular Ca^{2+} could affect the phosphorylation of myosin light chains (17,18,22). Following treatment with W-7, which is used as a calmodulin antagonist and an MLCK inhibitor (22), poly-L-Arg increased both the Papp of FD-4 and Gt and poly-L-Arg alone (see Fig. 4). These results suggest strongly that the promoting effect of poly-L-Arg on the solute TJ permeability is not involved in the contraction of perijunctional actin via MLCK activation following an increase in $[Ca^{2+}]_i$ (Fig. 6). Also, other MLCK activation-related processes such as the inhibition of MLC phosphatase by way of the activation of RhoK (23) may make a negligible contribution to the poly-L-Arg effect.

The presence of extracellular Ca^{2+} is important in maintaining TJ integrity (17,18). Recently, some reports have speculated that polycations displace Ca^{2+} from the intercellular junctions, resulting in disruption of the Ca^{2+}-dependent structures of cell-to-cell junctions (13,32). To investigate this possibility, we examined the effect of extracellular Ca^{2+} concentration on the poly-L-Arg-induced increase in TJ permeability. The results suggest that the increase in TJ permeability produced by poly-L-Arg is unrelated to the displacement or clearance of Ca^{2+} from the intercellular junctions, in particular adherens junctions, resulting in no induction of TJ disassembly (see Fig.2e). This was supported from a preliminary experiment; Ca^{2+} free in the bathing fluids produced an increase in Gt with a reduction in PD, enhancing the Papp of FD-4. Thus, it is evident that the intracellular signaling and extracellular events associated with Ca^{2+} don't lead to an increase in the Papp of FD-4 and Gt by poly-L-Arg.

Next, we investigated whether the phosphorylation and dephosphorylation of TJ proteins, which are believed to induce TJ assembly and disassembly, could affect the increase in Papp of FD-4 and Gt by poly-L-Arg (20–25,28,30,31). Pre-

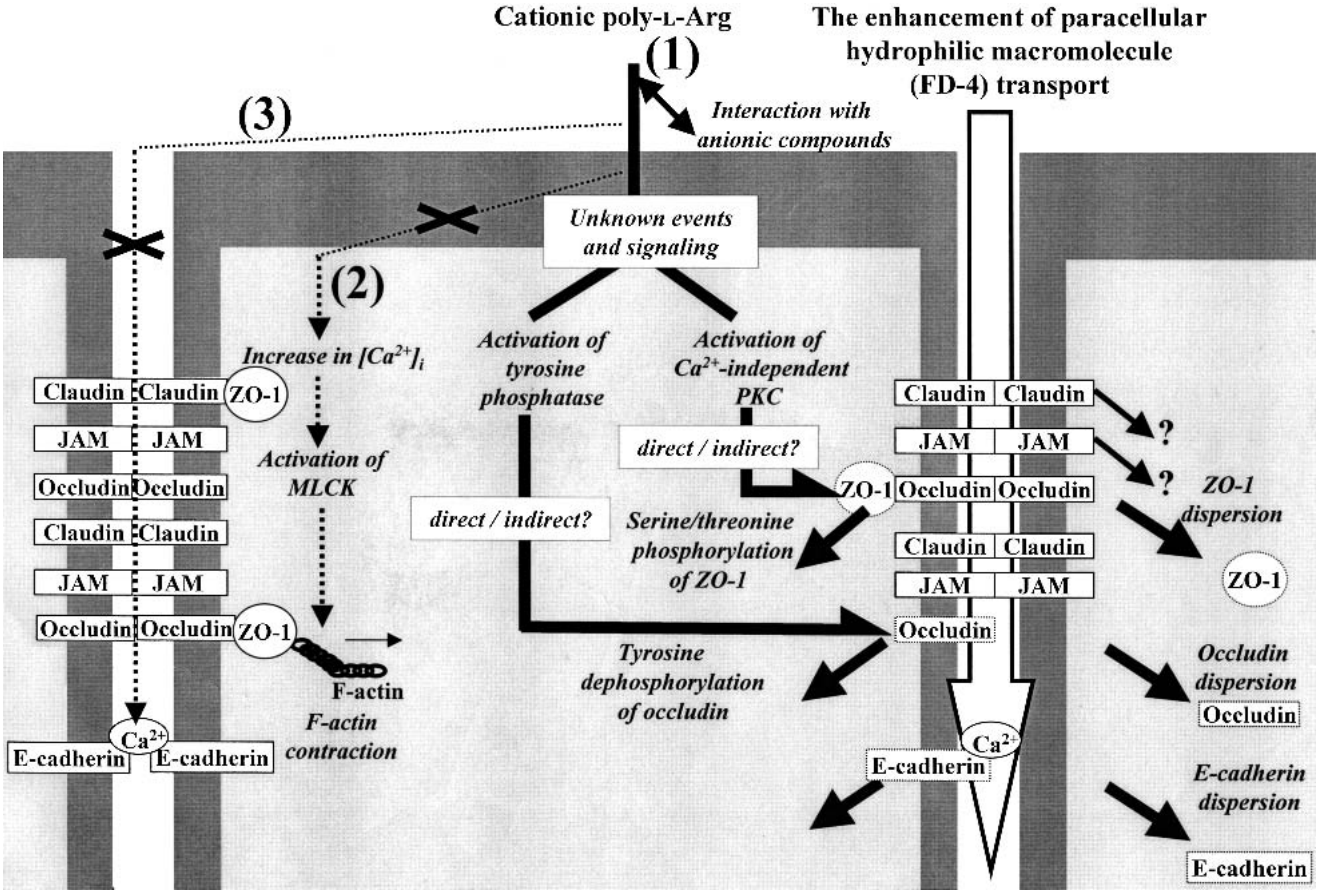

Fig. 6. Possible regulating mechanism of poly-l-Arg on the enhanced paracellular transport of macromolecules in rabbit nasal epithelium. (1): An ionic interaction of cationic poly-l-Arg with anionic components (molecules) on the epithelial cell surface may be trigger to enhance paracellular permeability (but not identified as specific molecule). The enhanced paracellular transport occurs via TJ disassembly associated, at least, with dispersion of ZO-1 and occludin and adherens junction disassembly (dispersion of E-cadherin). We provide the first evidence that poly-l-Arg leads to dispersion of ZO-1 and occludin via the serine/threonine phosphorylation of ZO-1 involving Ca^{2+}-independent PKC activation and tyrosine dephosphorylation, respectively. However, cellular events and signaling in the upper stream leading to dispersion of junction proteins is still unknown. (2): The promoting effect of poly-l-Arg on the solute TJ permeability is not involved in the contraction of perijunctional actin via MLCK activation following an increase in $[Ca^{2+}]_i$. (3): The increase in TJ permeability produced by poly-l-Arg is unrelated to the displacement and/or clearance of Ca^{2+} from the intercellular junctions, in particular adherens junctions. The direct action of poly-l-Arg to TJ proteins was found to be minor.

incubation with RTK inhibitor genistein (20), non-RTK inhibitor PP2 (21), MEK inhibitor PD98059 (24) and PI3K inhibitor LY294002 (25) indicate that there is no relationship to tyrosine phosphorylation of junction proteins including ZO-1 and occludin to poly-L-Arg effect (see Fig. 4). In addition, the results also indicate that the promoting effect of poly-L-Arg on the TJ permeability of FD-4 is unrelated to the tyrosine kinase cascade involving MEK or PI3K signaling pathway (20,21,24,25). In contrast, preincubation with the PKC inhibitor rottlerin (26) or Gö 6983 (27) significantly reduced the increase in Papp of FD-4 by poly-L-Arg. Increased Gt also tended to be reduced to a degree, although there was no significant difference between inhibitor treatment vs. no treatment (for rottlerin; $p = 0.18$, for Gö 6983; $p = 0.29$) (Fig. 4). Recently, it has been shown that the Ca^{2+}-independent PKC isoforms λ and ζ (atypical PKC) are localized to the cell junction complex in the MDCK cell monolayers (33). Hence, our results show that poly-L-Arg may activate the Ca^{2+}-independent PKC, but not Ca^{2+}-dependent PKC in rabbit nasal epithelium because of it being unrelated to $[Ca^{2+}]_i$ alteration, thereby allowing phosphorylation of junction proteins, especially serine/threonine residues. On the other hand, both the poly-L-Arg-induced increase in Papp of FD-4 and Gt were significantly suppressed by the tyrosine phosphatase inhibitor dephostatin (29), whereas the serine/threonine phosphatase inhibitor okadaic acid had no effect (28) (Fig. 4), deriving the tyrosine dephosphorylation of TJ proteins, but not serine/threonine dephosphorylation. These results indicate that both the PKC activation and tyrosine dephosphorylation induced by poly-L-Arg significantly reduces TEER and increases the paracellular permeability of FD-4 (see Fig. 6). However, we cannot estimate simultaneously the PKC activation and tyrosine dephosphorylation induced by poly-L-Arg, because of the induction of epithelial cell death following co-incubation of rottlerin or Gö 6983 with dephostatin under these experimental conditions.

Furthermore, we evaluated the effect of poly-L-Arg on the distribution of ZO-1 and occludin involving these activation processes using immunofluorescent localization. As shown in Fig. 5, poly-L-Arg induces occludin disassembly by way of tyrosine dephosphorylation as well as ZO-1 dispersion via serine/threonine phosphorylation. Overall, we provide the first evidence that poly-L-Arg leads to TJ disassembly with both the tyrosine dephosphorylation of occludin and the serine/threonine phosphorylation of ZO-1 involving Ca^{2+}-independent PKC activation, resulting enhanced paracellular transport of macromolecules with a reduction in TEER (see Fig. 6). Further investigations are necessary to estimate the tyrosine dephosphorylation and serine/threonine phosphorylation levels of occludin and ZO-1, respectively, to confirm these results. With respect to TJ disassembly involving enhanced paracellular transport, the alteration in localization of claudin should be also determined following poly-L-Arg exposure because of an important integral component of TJ strand (34). In our earlier study, an ionic interaction of cationic poly-L-Arg with anionic components on the epithelial cell surface may be a trigger to enhance the paracellular transport as shown in Fig. 6 (35). In addition, the regulatory mechanism of the poly-L-Arg effect is likely to be dependent on energy-requiring cellular processes while acting only on the apical membrane components [12]. These processes also led to alteration in the localization of E-cadherin. However, cellular events and signaling in the upper stream which induce TJ disassembly-relating events, including serine/threonine phosphorylation of ZO-1 involving Ca^{2+}-independent PKC activation and tyrosine dephosphorylation of occludin following poly-L-Arg exposure still remain unknown (see Fig. 6).

We conclude that poly-L-Arg enhances the paracellular permeability of macromolecules by way of serine/threonine phosphorylation of ZO-1 involving Ca^{2+}-independent PKC activation and tyrosine dephosphorylation of occludin in rabbit nasal epithelium. Such phosphorylation and dephosphorylation leads to the dispersion of junction proteins, in particular ZO-1 and occludin, into the cytoplasm, followed possibly by TJ disassembly. These findings provide useful information for the development of transnasal delivery systems for macromolecules with polycationic materials as promoters of solute transport and should encourage further investigations including a search for the likely intracellular signaling processes.

ACKNOWLEDGMENT

The authors thank Professor Akira Shirahata (Laboratory of Cellular Physiology, Faculty of Pharmaceutical Sciences, Josai University) for helpful discussions and useful comments, and for assistance with the manuscript. This work was supported in part by the Japan Science and Technology Corporation.

REFFRENCES

1. M. Cereijido, J. Valdes, L. Shoshani, and R. G. Contreras. Role of tight junctions in establishing and maintaining cell polarity. *Annu. Rev. Physiol.* **60**:161–177 (1998).
2. J. L. Madara. Regulation of the movement of solutes across tight junctions. *Annu. Rev. Physiol.* **60**:143–159 (1998).
3. A. Fasano. Novel approaches for oral delivery of macromolecules. *J. Pharm. Sci.* **87**:1351–1356 (1998).
4. H. Clarke, C. W. Marana, A. Peralta Soler, and J. M. Mullin. Increased tight junction permeability can result from protein kinase C activation/translocation and act as a tumor promotional event in epithelial cancers. *Adv. Drug Deliv. Rev.* **41**:283–301 (2000).
5. G. T. A. McEwan, M. A. Jepson, B. H. Hirst, and N. L. Simmons. Polycation-induced enhancement of epithelial paracellular permeability is independent of tight junctional characteristics. *Biochim. Biophys. Acta.* **1148**:51–60 (1993).
6. H. Natsume, S. Iwata, K. Ohtake, M. Miyamato, M. Yamaguchi, K. Hosoya, D. Kobayashi, K. Sugibayashi, and Y. Morimoto. Screening of cationic compounds as an absorption enhancer for nasal drug delivery. *Int. J. Pharm.* **185**:1–12 (1999).
7. M. Hammes and A. Singh. Effect of polycations on permeability of glomerular epithelial cell monolayers to albumin. *J. Lab. Clin. Med.* **123**:437–446 (1994).
8. L. Illum, N. F. Farrai, and S. S. Davis. Chitosan as a novel nasal delivery system for peptide drugs. *Pharm. Res.* **11**:1186–1189 (1994).
9. N. G. M. Schipper, S. Olsson, J. A. Hoogstraate, A. G. de Boer, and K. M. Varum. Chitosans as absorption enhancers for poorly absorbable drugs 2: mechanism of absorption enhancement. *Pharm. Res.* **14**:923–929 (1997).
10. A. F. Kotze, H. L. Lueβen, B. J. Leeuw, A. G. de Boer, J. C. Verhoef, and H. E. Junjinger. *N*-trimethyl chitosan chloride as a potential absorption enhancer across mucosal surfaces: in vitro evaluation in intestinal epithelial cells (Caco-2). *Pharm. Res.* **14**: 1197–1202 (1997).
11. K. Ohtake, H. Natsume, H. Ueda, and Y. Morimoto. Analysis of transient and reversible effects of poly-L-arginine on the in vivo nasal absorption of FITC-dextran in rats. *J. Control. Rel.* **82**:263–275 (2002).
12. K. Ohtake, T. Maeno, H. Ueda, H. Natsume, and Y. Morimoto.

Poly-L-Arginine predominantly increases the paracellular permeability of hydrophilic macromolecules across rabbit nasal epithelium in vitro. *Pharm. Res.* **20**:153–160 (2003).
13. G. Ranaldi, I. Marigliano, I. Vespignani, G. Perozzi, and Y. Sambuy. The effect of chitosan and other polycations on tight junction permeability in the human intestinal Caco-2 cell line. *J. Nutr. Biochem.* **13**:157–167 (2002).
14. E. Waelkens, J. Goris, and W. Merlevede. Activation of PCSM-protein phosphatase by Ca^{2+}-dependent protease. *FEBS Lett.* **192**:317–320 (1985).
15. Y. Biener and Y. Zick. Basic polycations activate the insulin receptor kinase and a tightly associated serine kinase. *Euro. J. Biochem.* **194**:243–250 (1990).
16. P. S. Leventhal and P. J. Bertics. Activation of protein kinase C by selective binding of arginine-rich polypeptide. *J. Biol. Chem.* **268**:3906–3913 (1993).
17. S. T. Ballard, J. H. Hunter, and A. E. Taylor. Regulation of tight-junction permeability during nutrient absorption across the intestinal epithelium. *Annu. Rev. Nutr.* **15**:35–55 (1995).
18. B. M. Denker and S. K. Nigam. Molecular structure and assembly of the tight junction. *Am. J. Physiol.* **274**:F1–F9 (1998).
19. J. E. Merritt, W. P. Armstrong, C. D. Benham, T. J. Hallam, R. Jacob, A. Jaxa-Chamiec, B. K. Leigh, S. A. McCarthy, K. E. Moores, and T. J. Rink. SK&K 96365, a novel inhibitor of receptor-mediated calcium entry. *Biochem. J.* **271**:515–522 (1990).
20. T. Tsukamoto and S. Nigam. Role of tyrosine phosphorylation in the reassembly of occludin and other tight junction proteins. *Am. J. Physiol.* **276**:F737–F750 (1999).
21. M. C. Chen, T. E. Solomon, E. Perez Salazar, R. Kui, E. Rozengurt, and A. H. Soll. Secretin regulates paracellular permeability in canine gastric monolayers by Src kinase-dependent pathway. *Am. J. Physiol.* **283**:G893–G899 (2002).
22. J. R. Turner, J. M. Angle, E. D. Black, J. L. Joyal, D. B. Sacks, and J. L. Madara. PKC-dependent regulation of transepithelial resistance: roles of MLC and MLC kinase. *Am. J. Physiol.* **277**:C554–C562 (1999).
23. S. V. Walsh, A. M. Hopkins, J. Chen, S. Narumiya, C. A. Parkos, and A. Nusrat. Rho kinase regulates tight junction function and is necessary for tight junction assembly in polarized intestinal epithelia. *Gastroenterology* **121**:566–579 (2001).
24. Y. Chen, G. Lu, E. E. Schneeberger, and D. A. Goodenough. Restoration of tight junction structure and barrier function by down-regulation of the mitogen-activated protein kinase pathway in ras-transformed Madin-Darby canine kidney cell. *Mol. Biol. Cell* **11**:849–862 (2000).
25. P. L. Woo, D. Ching, Y. Guan, and G. L. Firestone. Requirement for Ras and phosphatidylinositol 3-kinase signaling uncouples the glucocorticoid-induced junctional organization and transepithelial electrical resistance in mammary tumor cells. *J. Biol. Chem.* **274**:32818–32828 (1999).
26. M. Gschwendt, H. J. Mueller, K. Kielbassa, R. Zang, W. Kittstein, G. Rincke, and F. Marks. Rottlerin, a novel protein kinase inhibitor. *Biochem. Biophys. Res. Commun.* **199**:93–98 (1994).
27. M. Gschwendt, S. Dieterich, J. Rennecke, W. Kittstein, H. J. Mueller, and F. J. Johannes. Inhibition of protein kinase μ by various inhibitors. Differentiation from protein kinase c isoenzymes. *FEBS Lett.* **392**:77–80 (1996).
28. K. L. Singer, B. R. Stevenson, P. L. Woo, and G. L. Firestone. Relationship of serine/threonine phosphorylation/dephosphorylation signaling to glucocorticoid regulation of tight junction permeability and ZO-1 distribution in nontransformed mammary epithelial cells. *J. Biol. Chem.* **269**:16108–16115 (1994).
29. M. Imoto, H. Kakeya, T. Sawa, C. Hayashi, M. Hamada, T. Takeuchi, and K. Umezawa. Dephostatin, a novel protein tyrosine phosphatase inhibitor produced by Streptomyces. I. Taxonomy, isolation, and characterization. *J. Antibiot. (Tokyo)* **46**:1342–1346 (1993).
30. J. Karczewski and J. Groot. Molecular physiology and pathophysiology of tight junctions III. Tight junction regulation by intracellular messengers: differences in response within and between epithelia. *Am. J. Physiol.* **279**:G660–G665 (2000).
31. J. M. Mullin, K. V. Laughlin, N. Ginanni, C. W. Marano, H. M. Clarke, and A. Peralta Soler. Increased tight junction permeability can result from protein kinase C activation/translocation and act as a tumor promotional event in epithelial cancers. *Ann. NY Acad. Sci.* **915**:231–236 (2000).
32. D. A. Uchida, C. G. Ballowe, and G. R. Cott. Cationic proteins increase the permeability of cultured rabbit tracheal epithelial cells: modification by heparin and extracellular calcium. *Exp. Lung Res.* **22**:85–99 (1996).
33. V. Dodane and B. Kachar. Identification of isoforms of G proteins and PKC that colocalize with tight junctions. *J. Membrane. Biol.* **149**:199–209 (1996).
34. M. Furuse, K. Fujita, T. Hiiragi, K. Fujimoto, and S. Tsukita. Claudin-1 and –2: novel integral membrane proteins localizing at tight junctions with no sequence similarity to occludin. *J. Cell Biol.* **141**:1539–1550 (1998).
35. M. Miyamoto, H. Natsume, S. Iwata, K. Ohtake, M. Yamaguchi, D. Kobayashi, K. Sugibayashi, M. Yamashina, and Y. Morimoto. Improved nasal absorption of drugs using poly-L-arginine on the nasal absorption of fluorescein isothiocyanate-dextran in rats. *Eur. J. Pharm. Biopharm.* **52**:21–30 (2001).